Vol. 1, No. 2 (2022) 74-80 http://sniqba.com.mx/revsniqba-2022-02-11/

Revista SNIQBA

ESTUDIO DE LA DINÁMICA DE REORIENTACION MOLECULAR EN *meso*-FENIL BODIPYs POR ESPECTROSCOPIA RMN

STUDY OF THE MOLECULAR REORIENTATION DYNAMICS IN *meso*-PHENYL BODIPYs BY NMR SPECTROSCOPY

Celín Lozano-Pérez*, Román Torres, Eduardo Arias, Ivana Moggio, Raquel Ledezma

Centro de Investigación en Química Aplicada, Blvd. Ing. Enrique Reyna No. 140, Saltillo, Coahuila. C.P. 25294. México

celin.lozano86@gmail.com, eduardo.arias@ciqa.edu.mx, ivana.moggio@ciqa.edu.mx

Received September 30, 2022; Revised: December 09, 2022; Accepted December 13, 2022

Resumen

Los rotores moleculares fluorescentes (FMR) a base de BODIPY se pueden usar como sensores de temperatura o viscosidad debido a que la rotación intramolecular modula la intensidad o el tiempo de vida de la emisión. Además, por estudios de anisotropía de fluorescencia, la reorientación molecular se puede evaluar mediante el tiempo de relajación longitudinal (T_1) por RMN. Este trabajo se enfoca en estudiar la reorientación molecular de BODIPYs con grupos *meso* fenilo con rotación restringida o libre mediante RMN. Específicamente, se calcularon T_1 de los núcleos de ^{1}H y ^{13}C al variar la temperatura de 300 K a 240 K y se calcula el tiempo de correlación rotacional (τ_c) y la energía de activación de reorientación rotacional (E_a) basándose en la teoría Bloembergen-Purcell-Pound (BPP). Además, se calcularon los valores de desplazamiento químico teóricos mediante GIAO-DFT con alta correlación (R^2 ~0.99 en ^{1}H y R^2 ~0.97 en ^{13}C). Los valores de ^{1}H T_1 y ^{13}C T_1 se reducen al disminuir la temperatura sin llegar a un mínimo, y los valores de ^{1}H T_1 van de 1 a 10 s mientras que en ^{13}C T_1 van de 0.5 a 2 s. Las moléculas BODIPY presentan un eje principal de rotación a través del grupo *meso*-fenilo y se observó un movimiento anisotrópico en las moléculas con el grupo fenilo con rotación libre. Los parámetros derivados de la teoría BPP confirman la alta movilidad del grupo *meso*-fenilo con rotación libre. Estos resultados muestran la alta correlación entre la estructura y la dinámica de reorientación molecular medida por T_1 RMN.

Palabras clave: BODIPY, FMR, relajación T_1 RMN, GIAO-DFT.

Abstract

BODIPY-based fluorescent molecular rotors (FMR) can be used as temperature or viscosity sensors given that the intramolecular rotation can tailor the emission intensity or fluorescence lifetime. Besides fluorescence anisotropy, the molecular reorientation can be assessed by NMR longitudinal relaxation time (T_1). This work focuses on the study by NMR of the molecular reorientation of *meso*-phenyl BODIPY with free and restricted motion. Specifically, ^{1}H T_1 and ^{13}C T_1 were determined by temperature variation from 300 K to 240 K and rotational correlation time (τ_c) along with rotational reorientation activation energy (E_a), which were estimated by Bloembergen-Purcell-Pound (BPP) theory. Moreover, theoretical chemical shifts were calculated by GIAO-DFT with high correlation (R^2 ~ 0.99 ^{1}H and R^2 ~ 0.97 ^{13}C). The values of ^{1}H T_1 and ^{13}C T_1 diminish with the temperature decrease without reaching a minimum and ^{1}H T_1 values range from 1 to 10 s, while ^{13}C T_1 are from 0.5 to 2 s. BODIPYs show a main rotation axis across the *meso*-phenyl moiety and an anisotropic motion is observed in molecules with free rotation *meso*-phenyl groups. The derived parameters from BPP theory confirmed the high mobility of free rotation *meso*-phenyl groups. These results show the high correlation between structure and molecular reorientation dynamics measured by T_1 NMR.

Keywords: BODIPY, FMR, relaxation T_1 NMR

Introduction

BODIPY is a fluorophore with large absorption coefficients in the UV and visible-near infrared region, high fluorescence quantum yield and short fluorescent lifetime, parameters that can be modulated along with the functionalization in several positions [1]. These features show the potential of BODIPYs as molecular fluorescent rotors (FMRs) [2]. FMRs have been developed as viscosity and/or temperature sensors given that the intramolecular rotation can tailor the emission intensity or lifetime [3]. Recently, a systematic study showed that *meso*-phenyl BODIPY molecular rotors with bromine, ester or amide groups are affected by environmental parameters such as temperature, viscosity, or polarity [4,5]. Moreover, BODIPY molecular rotors in high viscosity solvents have a high energy barrier, which hinders rotation and enables fluorescence. Conversely, low viscosity solvents allow rotation in BODIPY molecular rotors, which creates non-radiative de-excitation pathways impeding the fluorescence [2]. Although most literature in BODIPY molecular rotors assesses the molecular reorientation in FMRs by fluorescence techniques, NMR spectroscopy can also be used to further study this phenomenon. NMR spectroscopy is a powerful tool to determine the longitudinal relaxation time (T_1), which can be affected by several factors such as electronic effects, molecular mobility, and intermolecular interactions [6–9]. T_1 measurements can show molecular reorientation, segmental and local interactions. Some reported T_1 values in *meso*-substituted BODIPYs with CF_3-terminated alkyl chains are between 2-5 s [10]. However, there are few works that compare the molecular reorientation of *meso*-substituted BODIPY by T_1 NMR. Therefore, this work studies the molecular reorientation dynamics of three *meso*-substituted BODIPYs (Fig. 1) by ^{1}H T_1 and ^{13}C T_1 and derived parameters from the Bloembergen-Purcell-Pound (BPP) theory.

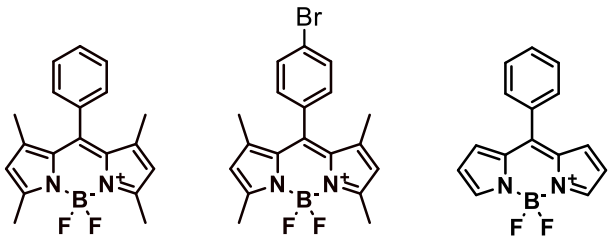

Fig. 1. *Meso-phenyl BODIPYs studied in this work.*

Experimental

All chemicals and reagents, from Sigma-Aldrich, were used as received without further purification. The reagents used to synthesize **BD**, **BDBr** and **BDR** (Fig. 1), according to literature procedures, were, benzoyl chloride and 2,4 dimethylpyrrole; 4-bromo benzoyl chloride and 2,4, dimethylpyrrole, benzoyl chloride and pyrrole, respectively. In brief, the reagents were dissolved in fleshly distilled dichloromethane and stirred for 18 h at room temperature. Then triethylamine and $BF_3{\cdot}Et_2O$ were added to the flask placed in an ice-water bath and stirred for 2 h. The solution was washed with distilled water, and brine and the organic layer was concentrated at low pressure. Column chromatography on silica gel (eluent: 1:1 dichloromethane: n-hexanes) provided the product as a red solid.

Chemical shift (δ) assignments of ^{1}H and ^{13}C experimental spectra were corroborated by computational chemistry with the Gauge-Including Atomic Orbital (GIAO) method. All DFT calculations were performed in ORCA Version 5.0.3 [11]. All the molecular geometries were optimized at def2-SVP/MN15 DFT level and the effects of chloroform were included by the conductor-like polarizable continuum model (CPCM). Shielding constants (σ) were calculated using pcSseg-2 basis set, a triple zeta basis set design for σ calculations, and PBE0 functional. Theoretical δ values were predicted by a linear scaling factor that correlates experimental δ with estimated σ by GIAO-DFT. The coefficient of determination (R^2) was used to assess the theoretical δ.

All NMR experiments were acquired in an AVANCE III HD 400 spectrometer (with a 5 mm multinuclear BBI-decoupling probe with Z grad) with resonance frequencies for ^{1}H and ^{13}C of 400.14 MHz and 100.61 MHz, respectively. Samples were dissolved in 5 mm Young tubes with $CDCl_3$ (~0.04 g/mL) and de-oxygenated by three freeze-pump-thaw cycles. Measurements were performed between 300 K and 240 K with 10 K cooling ramps and thermal equilibrium time of 300 s. At each temperature ramp, ^{1}H and ^{13}C spectra were acquired along with T_1 relaxation experiments. The variable delay list (VDLIST) was adjusted for each molecule such that the time interval was between 0.1 T_1 to 1.5 T_1. Typically, VDLIST was 0.1-3 s for both ^{1}H T_1 and ^{13}C T_1 given that only protonated carbons are investigated. The ^{1}H T_1 experiments with variable

temperature were acquired with delay time of 15 s (D1), a 16 K (TD2) x 10 (TD1) matrix of complex points and 2 accumulated transients per experiment increment. In the case of ^{13}C T_1, D1 = 6 s, the complex point matrix was 65 K (TD2) x 7 (TD1) with 180 accumulated transients per experiment increment. ^{1}H T_1 and ^{13}C T_1 data were processed by exponential filter with Fourier transform in F2 dimension with LB = 1Hz for ^{1}H and 3 Hz for ^{13}C. The integrals used for T_1 calculations in the inversion-recuperation method were performed in the T_1 module of the Dynamic Center software from Bruker using manual integration with one time-constant component.

T_1 values can be explained by a combination of relaxation mechanism. Typically, the relaxation mechanisms for nuclear spin systems are dipole-dipole interactions (DD), chemical shift anisotropy interactions (CSA), spin rotation (SR), scalar coupling (SC) and quadrupolar coupling (Q) [6]. In the case of nuclei with spin ½, contributions from SR, SC and Q can be negligible. The DD relaxation mechanism in ^{1}H depends mainly on inter or intramolecular neighbor protons. In contrast, ^{13}C T_1 relaxation is caused by intramolecular DD interactions of carbon-proton bonds. The Bloembergen-Purcell-Pound (BPP) theory provides the theoretical basis for describing the temperature dependence of T_1 observed as a function of the rotational correlation time (τ_c) and Larmor frequencies. Thus, BPP theory describes DD relaxation for ^{1}H and ^{13}C with the following equations:

$$\frac{1}{T_{1,H}} = A_{0,H}\left(\frac{\tau_c}{1+(\omega_H\tau_c)^2} + \frac{4\tau_c}{1+(2\omega_H\tau_c)^2}\right) \quad (1)$$

$$X = \left(\frac{\tau_c}{1+((\omega_H-\omega_C)\tau_c)^2} + \frac{3\tau_c}{1+(\omega_C\tau_c)^2} + \frac{6\tau_c}{1+((\omega_C+\omega_H)\tau_c)^2}\right) \quad (2)$$

$$\frac{1}{T_{1,C}} = A_{0,C}(X) \quad (3)$$

$$A_{0,H} = \frac{3N}{10}\left(\frac{\mu_0}{4\pi}\right)\gamma_H^4\hbar(r_{H-H}^{-6}) \quad (4)$$

$$A_{0,C} = \frac{N}{10}\left(\frac{\mu_0}{4\pi}\right)\gamma_C^2\gamma_H^2\hbar(r_{C-H}^{-6}) \quad (5)$$

Where A_0 constant is defined by the number of nuclei attached to the observed nuclei, μ_0 is the vacuum permeability, γ_H and γ_C are ^{1}H and ^{13}C gyromagnetic constants, h is the reduced Planck constant and r corresponds to the proton-proton or C-H distance.

The temperature dependence of the rotational correlation time (τ_c) is described by an Arrhenius-type equation.

$$\tau_C = \tau_0 exp\left(\frac{E_a}{RT}\right) \quad (6)$$

Where τ_0 is the pre-exponential factor, R is the ideal gas constant, T is the absolute temperature, E_a is the molecular reorientation activation energy. Typically, T_1 measurements as a function of temperature allow to determine a minimum, which can be correlated with A_0 given that this parameter is temperature independent. In case that a minimum in the temperature range is not observed, τ_c can be calculated by non-linear least squares [12].

Results and Discussion

The chemical structures of *meso*-phenyl BODIPYs were confirmed by ^{1}H and ^{13}C NMR spectroscopy. The chemical shift (δ) assignments were corroborated by GIAO-DFT where R^2 ~ 0.99 for ^{1}H and ~0.98 for ^{13}C. ^{1}H NMR spectra of **BD**, **BDBr** and **BDR** in Fig. 2 show similar peaks and intensities for **BD** and **BDBr**. For **BD** and **BDBr**, methyl protons H10 and H11 are at δ ~ 1.4 ppm and δ ~ 2.6 ppm, while methyne protons H2 are at δ ~ 6.0 ppm. In the case of **BDR**, methyne protons H1, H2 and H3 are shifted towards low field and located at 7.9, 6.6 and 6.9 ppm, respectively. In the aromatic region, phenyl protons of **BD** are observed as two small broad signals at 7.3 ppm (H7, 2H) and 7.5 ppm (H8 and H9, 3H); for **BDBr** phenyl protons are observed as an AA'BB' spin coupling system at 7.2 ppm (H7, d, J = 8.4 Hz, 2H) and 7.7 ppm (H8, d, J = 8.4 Hz, 2H); and a broad signal at 7.6 ppm (H7, H8 and H9, 5H) for **BDR**.

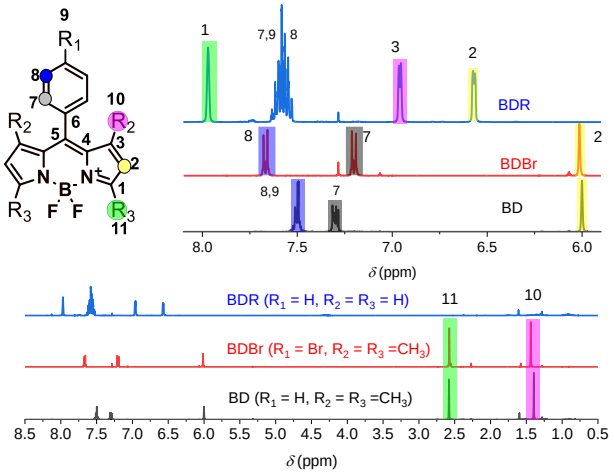

Fig. 2. ^{1}H spectra assignments for meso-phenyl BODIPYs.

The ^{13}C NMR assignment of protonated carbons (C2, C7, C8, C10 and C11) was confirmed by GIAO-DFT as shown in Fig. 3. The protonated carbons were

selected because they have higher intensity than quaternary carbons, which is important for ^{13}C T_1 measurements and parameter derivation with the BPP theory. C2 methyne carbons are observed as single peaks at $\delta \sim 121$ ppm for **BD** and **BDBr**, while for **BDR** C2 is shifted towards high field ($\delta \sim 118$ ppm). Methyl carbons (C10 and C11) of **BD** show two signals at δ~14.3 and 14.6 ppm, while for **BDBr** only one signal is observed at δ ~14.3 ppm. This behavior is also reproduced by theoretical δ calculations (GIAO-DFT) suggesting that the bromo-phenyl moiety has a deshielding effect over C10 which is also observed for the aromatic carbons C7 (δ~129.8 ppm) and C8 (δ ~132.4 ppm) in **BDBr** relative to carbons in **BD**. In **BDR**, C7, C8 and C9 are observed at δ~130.5, 128.4 and 130.7 ppm, respectively.

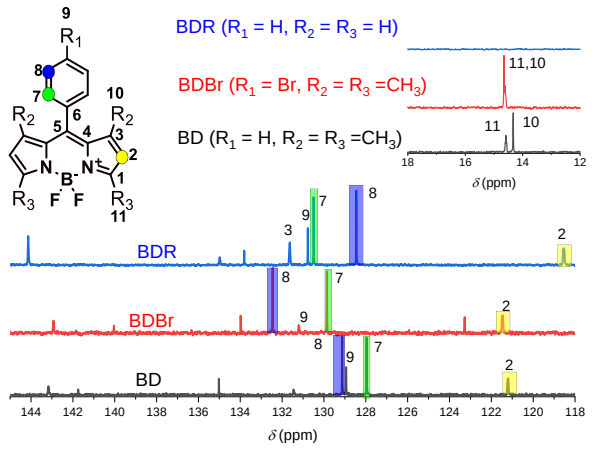

Fig. 3. ^{13}C spectra assignments for meso-phenyl BODIPYs.

The ^1H T_1 and ^{13}C T_1 temperature dependence, Fig. 4, in *meso*-phenyl BODIPY analogues, shows that T_1 values diminish with the temperature decrease without reaching a minimum. The absence of a minimum in the range of 300 K to 240 K indicates that the observed nuclei show free rotation along Z axis and the solvent is non-viscous [13,14] . For example, Fig. 4a shows the temperature dependence of **BD** from 300 K to 240 K. At 300 K, ^1H T_1 of H11 and H10 in **BD** is ~ 1.7 s and T_1 values for H7, H8 and H9 are 3.2-4.3 s and for H2 T_1 = 5.3 s. The short ^1H T_1 values in methyl groups are explained by a combination of spin-rotation and the dipolar relaxation mechanism where SR is the dominant mechanism [13]. Thus, methyl groups in **BD** show fast and unrestrained rotational motions with efficient SR relaxation at RT and high temperatures, which means shorter T_1 [14]. The long T_1 in H2 is also dominated by a combination of DD and SR mechanism since the closer protons are in the methyl groups and DD relaxation becomes ineffective. It can also be argued that **BD** tumbles rapidly in solution due to the small molecular weight. Therefore, the dipole-dipole relaxation in H2 is not effective and T_1 becomes longer. In the aromatic region, T_1 of H8 and H9 are shorter than the one in H7 suggesting that H9 is over the rotational axis. However, the strong spin-spin coupling (J) in the aromatic region limits further discussion of the molecular motion. Thus, ^{13}C T_1 measurements were performed given that the principal relaxation mechanism in carbons with directly attached protons is dipole-dipole mechanism.

Fig. 4b shows the temperature dependence of ^{13}C T_1 in **BD**, which shows similar features as ^1H curves. At 300 K, ^{13}C T_1 of C10 and C11 are around 1.8 s; for C2, C7, C8 and C9 ^{13}C T_1 is 1.3, 1.2, 1.3 and 1.1 s, respectively.

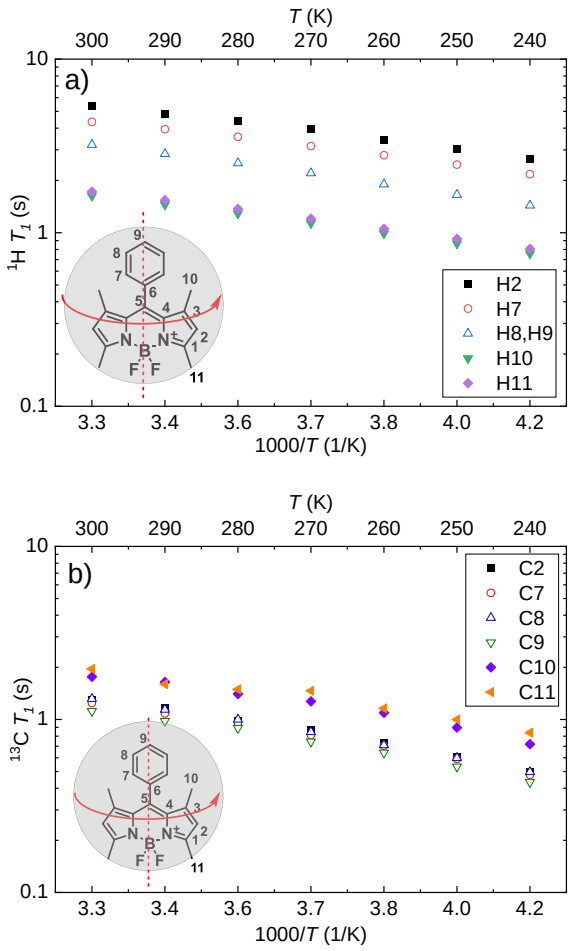

Fig. 4. Temperature dependence of BD. a) ^1H T_1 and b) $^{13}CT_1$. Inset: Proposed rotational motion of BD.

In this case, the fast and unrestricted motion of methyl groups is represented by long T_1 (1.8 s) given that DD relaxation is less effective, while the phenyl moiety shows effective DD relaxation (shorter T_1). ^{13}C T_1 in C9 is the shortest T_1 compared to C2, C7 and C8. This is because rotation around the axis is fast and causes inefficient relaxation (long T_1) for the off-axis carbons. With the results from ^{1}H T_1 and ^{13}C T_1, we propose that **BD** behaves as a sphere with an isotropic rotational motion where C9 and B atom are in the rotational axis and C2 is the farthest off-axis carbon, insets in Fig. 4.

Fig. 5 shows the comparison of ^{1}H T_1 and ^{13}C T_1 vs temperature of selected atoms in **BD**, **BDBr** and **BDR** where T_1 values diminish with temperature decrease. This behavior is characteristic of small molecules in non-viscous solvents. Here, the relaxation is less efficient with overall rapid molecular rotation and as the temperature diminishes, the relaxation becomes more effective and T_1 shortens.

In Fig. 5a, ^{1}H T_1 of phenyl protons (H7, H8 and H9) in **BDR** are twice the ones in **BD**, which has almost the same ^{1}H T_1 as **BDBr**. This behavior indicates that the phenyl group in **BDR** rotates faster than the ones in **BD** or **BDBr** because of the absence of methyl groups that hinder the phenyl rotation. Moreover, ^{1}H T_1 of H2 in all of the molecules is longer than the ones in the phenyl moiety suggesting that H2 rotates rapidly, and it is the farthest from the rotation axis. Thus, ^{1}H T_1 measurements indicate that **BD** and **BDBr** have the same rotational speed but rotation in **BDR** is even faster. Thus, if a small molecule tumbles rapidly, the DD relaxation is less effective and T_1 becomes longer.

The ^{13}C T_1 measurements of **BD**, **BDBr** and **BDR** in Fig. 5b corroborates the behavior observed by ^{1}H T_1 measurements. ^{13}C T_1 of C2 of the **BDBr** exhibits the shortest value while the ones in **BDR** have the longest. Therefore, the rotational speed of the molecules is as follows **BDR** > **BD** > **BDBr**. Moreover, ^{13}C T_1 values of the phenyl carbons (C7, C8 and C9) indicate that the rotational speed of these carbons is like that in C2, except for **BDR**, which is higher. Thus, **BDBr** has an isotropic motion like **BD** while **BDR** presents an anisotropic motion where the phenyl moiety rotates faster that the BODIPY fragment.

Assuming that the dipole-dipole relaxation mechanism is the only one that contributes to the ^{13}C relaxation times of protonated carbons, Table 1 shows the ^{13}C T_1 derived parameters (τ_0 and E_a) from the BPP theory (eq. 1-6). BPP parameters were grouped in protonated carbons in the pyrrolic rings, the phenyl ring and methyl groups. Regardless of the absence of a minimum in the ^{13}C T_1 *vs* temperature curves, all protonated carbons T_1 values fit well the Arrhenius-type BPP behavior.

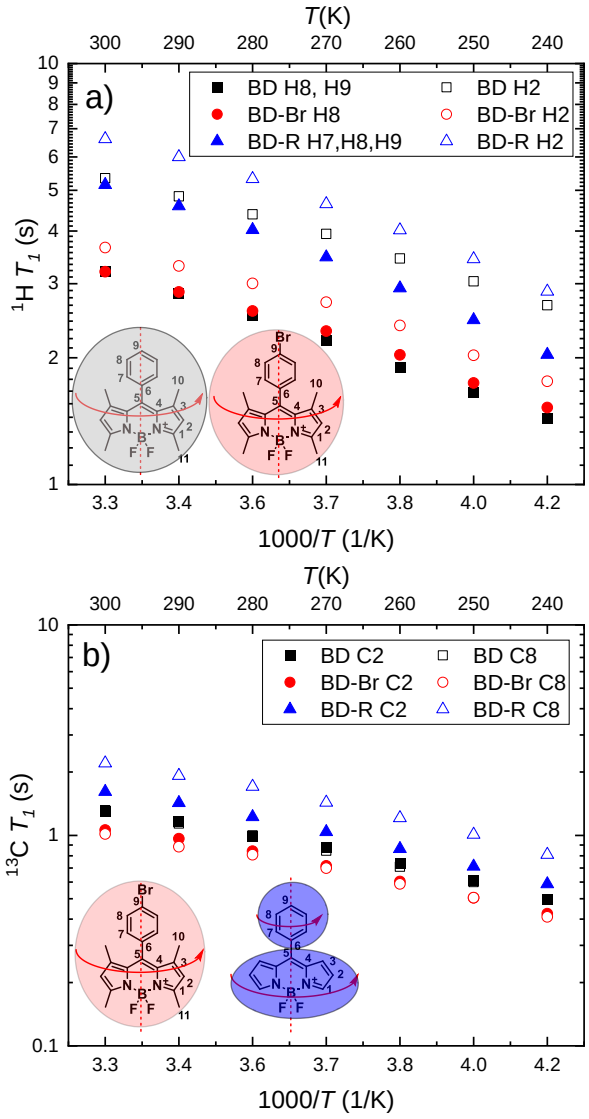

Fig. 5. Comparison of selected T_1 values as a function of temperature a) $^{1}HT_1$ and b) $^{13}CT_1$. Inset: Proposed rotational motion of **BD**, **BDBr** and **BDR**.

The mean correlation time (τ_c) values at 300 K calculated by eq 6 with τ_0 and E_a values from ^{13}C T1 experiments are shown in Table 1. τ_c values of the protonated carbons in the pyrrolic rings and phenyl ring are similar, $\tau_c = 1.25 \times 10^{-11}$ s for **BD** y $\tau_c = 7.65 \times 10^{-12}$ s para **BDBr**.

Conversely, the phenyl group (τ_c = 8.6 x 10^{-12} s) of **BDR** has τ_c at 300 K faster that the pyrrolic rings (τ_c = 1.0 x 10^{-11} s). In the case of proximal and distal methyls in **BD** and **BDBr**, the mean τ_c at 300 K is 2.8 x 10^{-12} s and 1.7 x 10^{-12} s, respectively. These values are typical for small molecules in non-viscous solutions [15].

Table 1. Derived parameter from BPP theory for meso-phenyl BODIPYs.

atom	BD		BDBr		BDR	
	E_a (kJ/mol)	τ_0 x 10^{-13} (s)	E_a (kJ/mol)	τ_0 x 10^{-13} (s)	E_a (kJ/mol)	τ_0 x 10^{-13} (s)
Pyrrolic rings						
1	---	---	---	---	10.4	1.72
2	9.5	2.60	9.8	1.46	10.2	1.59
3	---	---	---	---	10.2	1.76
Mean	9.50	2.60	9.80	1.46	10.3	1.69
τ_c x 10^{-12} (s) At 300 K	11.7		7.4		10.4	
Phenyl group						
7	9.8	2.29	9.3	1.75	9.7	1.39
8	9.4	2.89	8.8	2.26	9.8	1.37
9	9.3	3.37	---	---	9.8	2.27
Mean	9.50	2.85	9.0	2.0	9.8	1.67
τ_c x 10^{-12} (s) At 300 K	12.9		7.5		8.4	
Methyl groups						
10	8.60	0.91	8.4	0.59	---	---
11	7.90	1.13	8.4	0.59	---	---
Mean	8.25	1.02	8.4	0.59	---	---
τ_c x 10^{-12} (s) At 300 K	2.8		1.7		---	

The activation energies (E_a) of the molecular reorientation of phenyl carbons are around 9.5 kJ/mol for **BD**, 9.0 kJ/mol for **BDBr** and 9.8 kJ/mol for **BDR** while the ones for the carbons in the pyrrolic rings are 9.5, 9.8 and 10.3 kJ/mol, respectively. These results indicate that the reorientation mediated by the rotation of the phenyl group in **BDR** is faster than the one in the pyrrolic rings. Additionally, the relative high energy barrier in the pyrrolic rings of **BDR** is attributed to the anisotropic rotation. These E_a values are like ^{13}C T_1 studies in ionic liquids where fluctuations of functional groups and methyl rotations were present [12,16]**.** Moreover, E_a values in T_1 relaxation studies are associated to molecular confinement measurements, intermolecular interactions, and environmental effects around the molecule [17].

Conclusion

Calculations with quantum chemistry by using GIAO-DFT level of theory allowed to assign protons and carbons with high agreement with experimental ^1H and ^{13}C spectra. The ^1H T_1 and ^{13}C T_1 relaxation measurements of *meso*-phenyl BODIPYs diminished with the temperature decrease without reaching a minimum in the range of 240-300 K. ^1H T_1 and ^{13}C T_1 measurement aided to propose a rotational model where the rotational axis is located between atom C9 and boron. Moreover, **BD** and **BDBr** rotate as a sphere with an isotropic rotational motion. However, **BDR** shows an anisotropic motion where the phenyl moiety has higher rotation speed compared to **BD** and **BDBr**. BPP theory was used considering dipole-dipole as the main T_1 relaxation mechanism and the derived parameters (τ_c and E_a) confirmed the isotropic and anisotropic motions found experimentally. The relative high reorientation energy barrier in **BDR** was associated to the anisotropic rotation.

Acknowledgments

We wish to acknowledge the Mexican National Council for Science and Technology CONACYT for the financial support through “Becas Nacionales”. This work was supported by U.S. Air Force Office of Scientific Research, grant FA9550-14-1-0253.

References

(1) Loudet, A.; Burgess, K. BODIPY Dyes and Their Derivatives: Syntheses and Spectroscopic Properties. Chem Rev 2007, 107 (11), 4891–4932.

(2) Liu, X.; Chi, W.; Qiao, Q.; Kokate, S. v.; Peña-Cabrera, E.; Xu, Z.; Liu, X.; Chang, Y.-T. Molecular Mechanism of Viscosity Sensitivity in BODIPY Rotors and Application to Motion-Based Fluorescent Sensors. ACS Sens 2020, 5 (3), 731–739.

(3) Miao, W.; Yu, C.; Hao, E.; Jiao, L. Functionalized BODIPYs as Fluorescent Molecular Rotors for Viscosity Detection. Front Chem 2019, 7 (November), 1–6.

(4) Liu, X.; Chi, W.; Gómez-Infante, A. de J.; Peña-Cabrera, E.; Liu, X.; Chang, Y. A Systematic Study on the Relationship Between Viscosity Sensitivity and Temperature Dependency of

BODIPY Rotors. Bull Korean Chem Soc 2021, 42 (1), 91–94.

(5) Vyšniauskas, A.; López-Duarte, I.; Duchemin, N.; Vu, T.-T.; Wu, Y.; Budynina, E. M.; Volkova, Y. A.; Peña-Cabrera, E.; Ramírez-Ornelas, D. E.; Kuimova, M. K. Exploring Viscosity, Polarity and Temperature Sensitivity of BODIPY-Based Molecular Rotors. Physical Chemistry Chemical Physics 2017, 19 (37), 25252–25259.

(6) Wiedemann, C.; Hempel, G.; Bordusa, F. Reorientation Dynamics and Ion Diffusivity of Neat Dimethylimidazolium Dimethylphosphate Probed by NMR Spectroscopy. RSC Adv 2019, 9 (61), 35735–35750.

(7) Gradišek, A.; Cifelli, M.; Wojcik, M.; Apih, T.; Dvinskikh, S.; Gorecka, E.; Domenici, V. Study of Liquid Crystals Showing Two Isotropic Phases by 1H NMR Diffusometry and 1H NMR Relaxometry. Crystals (Basel) 2019, 9 (3), 178.

(8) Norton, R. S.; Gregson, R. P.; Quinn, R. J. 13C N.M.R. Spin–Lattice Relaxation Time Measurements Determining the Major Tautomer of 1-Methylisoguanosine in Solution. J. Chem. Soc., Chem. Commun. 1980, No. 8, 339–341.

(9) Rodríguez-Molina, B.; Pérez-Estrada, S.; Garcia-Garibay, M. A. Amphidynamic Crystals of a Steroidal Bicyclo[2.2.2]Octane Rotor: A High Symmetry Group That Rotates Faster than Smaller Methyl and Methoxy Groups. J Am Chem Soc 2013, 135 (28), 10388–10395.

(10) Huynh, A. M.; Müller, A.; Kessler, S. M.; Henrikus, S.; Hoffmann, C.; Kiemer, A. K.; Bücker, A.; Jung, G. Small BODIPY Probes for Combined Dual 19F MRI and Fluorescence Imaging. ChemMedChem 2016, 11 (14), 1568–1575.

(11) Neese, F. Software Update: The ORCA Program System—Version 5.0. WIREs Computational Molecular Science 2022, 12 (5).

(12) Di Pietro, M. E.; Castiglione, F.; Mele, A. Polar/Apolar Domains' Dynamics in Alkylimidazolium Ionic Liquids Unveiled by the Dual Receiver NMR 1H and 19F Relaxation Experiment. J Mol Liq 2021, 322, 114567.

(13) Parker, R. G.; Jonas, J. Spin-Lattice Relaxation in Several Molecules Containing Methyl Groups. Journal of Magnetic Resonance (1969) 1972, 6 (1), 106–116.

(14) Wiedemann, C.; Hempel, G.; Bordusa, F. Reorientation Dynamics and Ion Diffusivity of Neat Dimethylimidazolium Dimethylphosphate Probed by NMR Spectroscopy. RSC Adv 2019, 9 (61), 35735–35750.

(15) Witt, R.; Sturz, L.; Dölle, A.; Müller-Plathe, F. Molecular Dynamics of Benzene in Neat Liquid and a Solution Containing Polystyrene. 13C Nuclear Magnetic Relaxation and Molecular Dynamics Simulation Results. J Phys Chem A 2000, 104 (24), 5716–5725.

(16) Shimizu, Y.; Wachi, Y.; Fujii, K.; Imanari, M.; Nishikawa, K. NMR Study on Ion Dynamics and Phase Behavior of a Piperidinium-Based Room-Temperature Ionic Liquid: 1-Butyl-1-Methylpiperidinium Bis(Fluorosulfonyl)Amide. J Phys Chem B 2016, 120 (25), 5710–5719.

(17) Foster, R. J.; Damion, R. A.; Ries, M. E.; Smye, S. W.; McGonagle, D. G.; Binks, D. A.; Radjenovic, A. Imaging of Nuclear Magnetic Resonance Spin–Lattice Relaxation Activation Energy in Cartilage. R Soc Open Sci 2018, 5 (7), 180221.